Impurity Effects on Pore Formation at Al_2O_3/Alloy Interfaces

P. Y. Hou

Materials Sciences Division
Lawrence Berkeley National Laboratory
Berkeley, CA 94720

Abstract

The adhesion of Al_2O_3 scales on commercial grade alloys that do not contain a reactive element is usually poor due to the presence of 10-50 wppm of sulfur impurity, and/or of pores that formed at the scale/alloy interface. Sulfur is usually believed to segregate to the interface to weaken the interfacial bonding and to stabilize interfacial pores. By using field emission scanning Auger microscopy, the distribution of sulfur on pores and on oxide imprinted areas at Al_2O_3/FeAl interfaces was precisely determined. Interfacial pore growth as a function of oxidation time was obtained from scanning electron microscopy (SEM) and atomic force microscopy (AFM) analyses. The effects of sulfur segregation, surface impurity and reactive elements on pore nucleation and growth are discussed.

Introduction

A characteristic feature of the oxidation process in several metals and alloys is the formation of pores at the oxide/metal interface or in the metal immediately below this interface. When the pore size and/or density reach a critical value, adhesion of the scale deteriorates resulting in scale spallation during cooling. The mechanism of pore formation has been a subject of extensive debates, but is still not understood. The flow of vacancies from the oxide has been suggested to condense at the oxide/metal interface to form interfacial voids [1,2], or to condense in the metal immediately below the scale to cause void formation there [3-5]. Harris [6], on the other hand, suggested that tensile stresses induced in the alloy by the compressive growth stress in the oxide caused voiding beneath the scale. Porosity in the substrate can also be due to an unequal diffusion of the alloying elements [7], i.e. the Kirkendall effect, or by the formation of gaseous species, such as CO_2, as in the case of Ni [8]. Vacancy condensation to from voids at the scale/alloy interface depends on the effectiveness of this boundary as a vacancy sink [9]. Many oxide/alloy interfaces are believed to be good sinks where vacancies become annihilated [9,10]. Moreover, the oxide can often follow the retreating metal surface by plastic flow to avoid pore formation and scale separation [11].

Whatever the mechanism of pore formation, Grabke [12] suggested that interfacial voids are stabilized by the segregation of indigenous sulfur impurity from the alloy to the void surfaces. This segregation reduces the energy barrier for pore formation, hence facilitates the process. When sulfur is removed from the alloy by H_2-annealling [13,14], or tied up by the presence of a reactive element in the alloy [15,16], interfacial void formation seems to be greatly reduced. However, even with a reactive element in the alloy, very small pores, nm in diameter, could still be found at the very initial stages [17] or after prolonged oxidation [18]. Either these pores formed by different mechanisms, or the effect of sulfur is not so much on enhancing pore nucleation, but on stabilizing them to allow for their continued growth.

The purpose of this paper is to evaluate the effect of impurities on pore nucleation and growth. Sulfur in the alloy as well as possible surface contaminates are being considered.

Experimental

A Fe-40at%Al alloy containing 27.6 wppm of sulfur impurity, from Oak Ridge National Laboratory, was used for the study. The alloy was received as a ~ 1 mm thick hot-rolled sheet from an arc melted casting. It was annealed in He at 1100°C for 50 hours before cutting into 15mm x 10mm x 1mm sized coupons. Specimens were polished to a 1 μm finish with diamond paste and cleaned ultrasonically in acetone prior to oxidation in flowing, dry oxygen at 1000°C. A Cahn TGA system was used for thermogravimetric analysis. Other specimens were placed in an alumina boat with a thermocouple attached at the back of the specimen and oxidized in a horizontal furnace. After the desired oxidation time, which varied from 1 min to 24 hours, the boat and specimen were quickly pulled out of the furnace and cooled in ambient air. In both systems, the specimen temperature took about 10 minutes to reach 1000°C. One specimen surface was doped with a few drops of about $4x10^{-4}$ mole/l $NaNO_3$ solution to study its effect on pore formation.

Interfacial pores were examined using scanning electron microscopy (SEM) and atomic force microscopy (AFM) after the surface oxide was removed either by scratch

induced spallation or a strong adhesive. Chemical analyses of the alloy and oxide sides of the interface were carried out using conventional and field emission (FE) scanning Auger microscopy (SAM). With the conventional SAM (probe size about 1 μm), the oxidized specimen surface was scratched to cause scale spallation. This exposed both sides of the interface in the ultra high vacuum chamber, at about 10^{-10} torr [19]. In the FESAM (probe size of 30 nm), the parking stage arm inside the chamber was used to remove spallation prone scales to expose the alloy surface [20]. Compositions of the initially formed scales were determined using Auger depth profiling. Structure of the scale was studied using X-ray diffraction and its morphology examined by SEM.

Results and Discussions

Scale Development and Sulfur Segregation. Before impurity effects on pore formation can be determined, it is important to first examine how sulfur from the alloy segregates to the scale /alloy interface as the oxide grows. The surface of the Fe-40Al prior to oxidation contains a few nm thick native oxide that is composed of Fe, Al and O, as seen from the Auger depth profile shown in Fig. 1(a). As soon as the specimen is heated in O_2, the oxide thickens. After 1min, while the surface temperature was only 640°C, a scale richer in Fe near the outer surface and Al near the alloy surface developed (Fig. 1b). According to the work by Schumann et al [21] on the initial stage oxidation of NiAl, nucleation of transition phase alumina should have occurred at the scale/alloy interface during this time. Crystallization of the original native oxide is also expected [22], although it is not known how the two processes affect each other or pore nucleation. After 3 minutes in the furnace, the specimen temperature reached 910°C, and the scale consisted of an entire layer of Al_2O_3, identified by X ray diffraction as possibly θ-Al_2O_3. α-Al_2O_3 began to nucleate sporadically at the scale/alloy interface after 10 min oxidation (Fig 2a). After 1 hr, the entire alloy surface was covered with α-Al_2O_3 grain imprints (Fig. 2b), and the adjacent scale morphology had an equivalent α-Al_2O_3 grain size (Fig. 2c).

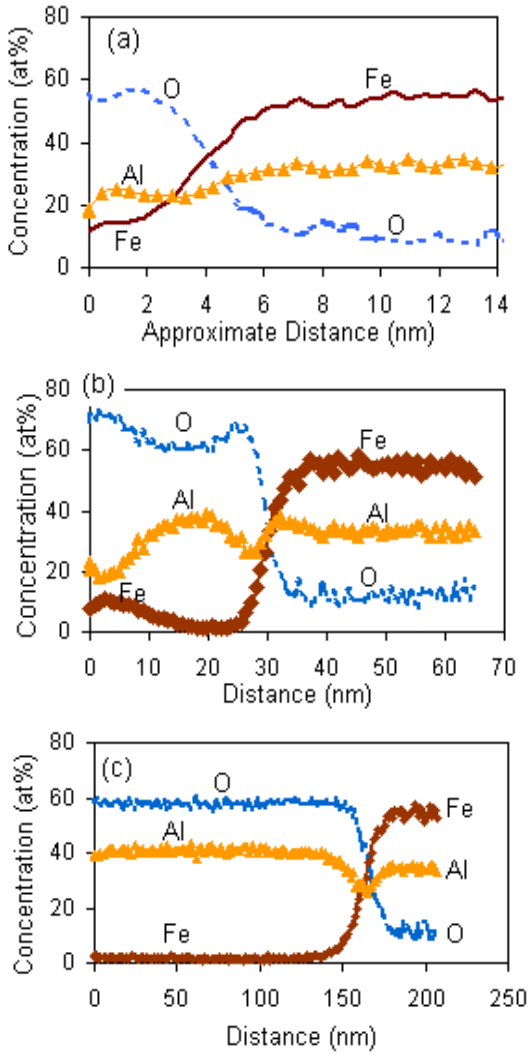

Figure 1: Auger depth profile of oxides on the surface of Fe40Al alloy after (a) 0 min, (b) 1 min and (c) 3 min oxidation. Specimen surface temperatures on (b) and (c) were 640 and 910°C respectively.

Different sizes of pores occasionally can be found on an otherwise smooth alloy surface beneath the scale after oxidation for 1 and 3 minutes; an example is given in Fig. 3 for a 3 min sample. The sub-micro sized pores became indistinguishable after the interface was covered with α-Al_2O_3 grains, but μm-sized ones are visible on every sample. The density of pores increased quickly during the first hour of oxidation, and the average pore size increased continually with oxidation time [23,24].

Sulfur was never present on the oxide side of the interface, where only Al and O were detected. The buildup of S with oxidation time on the metal side, on interfacial voids and on oxide-imprinted areas, is shown in Fig. 4. The smooth alloy surface under the transition alumina was free from any detectible impurities, but about 21 at% of sulfur was found by conventional SAM on the surfaces of all μm-sized pores, such as those seen on the left hand side of Fig. 3. Sulfur began to be detected on the interface after it was covered with α-Al_2O_3. This segregation behavior is not limited by S diffusion in the alloy, since S readily segregated to the pore surfaces, which are essentially free surfaces beneath the oxide scale. More S was detected at the interface by conventional SAM than by FE SAM, because the 1 μm probe size of the former included several oxide grain imprints whose average size is only about 0.3 μm (see Fig. 2b). Pores that may exist between the oxide grains are expected to have a high amount of sulfur on them, hence would contribute to the final analysis. Using a 30 nm probe of the FE SAM, individual facets of the oxide grain imprint could be analyzed, and *every one* of them contained sulfur. This result showed unambiguously that sulfur segregated to intact α-Al_2O_3/alloy interface. The large error bar after longer times is a result of the variations of sulfur content on different facets [20]. It is not known why similar segregation did not occur at the transition alumina/alloy interface. One likely explanation is that the excess

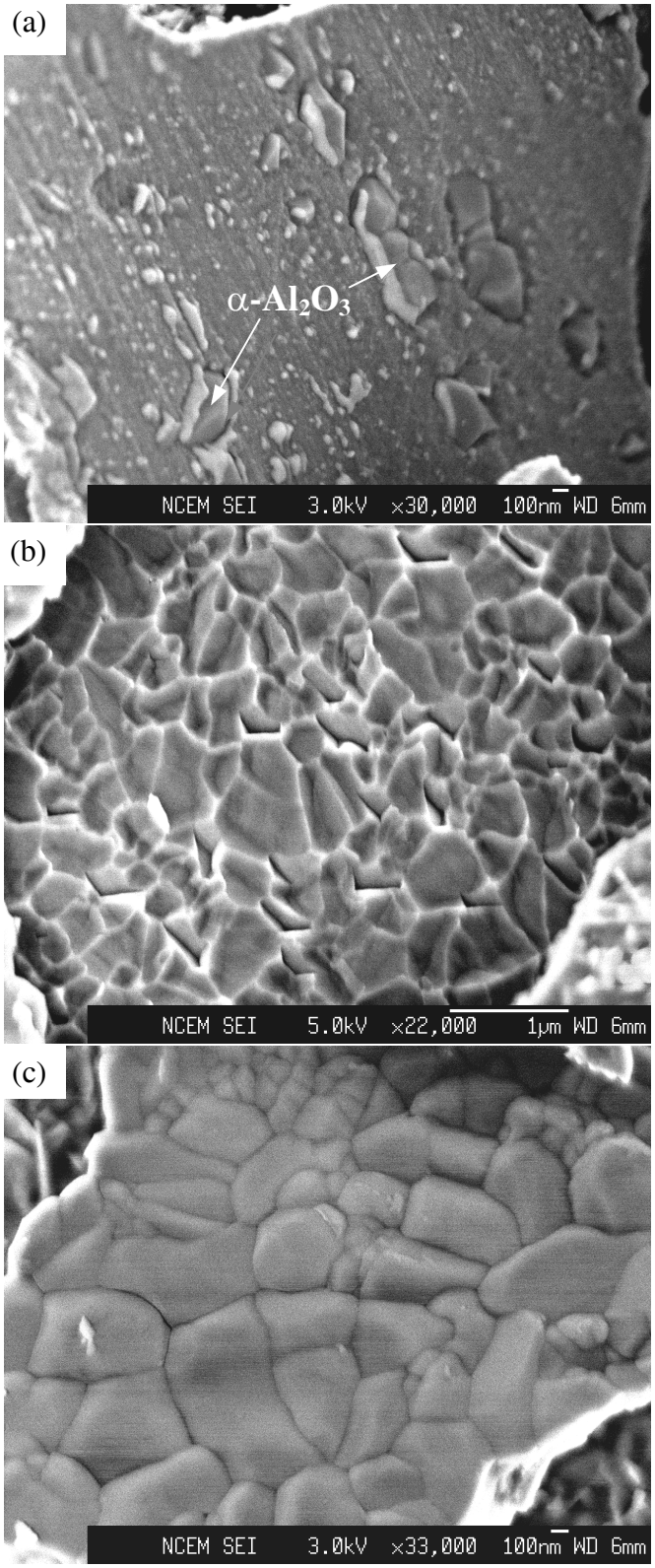

Figure 2: SEM micrographs of (a) underside of a 10 min scale. (b) Alloy and (c) oxide underside respectively of scale formed after 1hr oxidation.

free energy of interfacial segregation depends strongly on interface microstructure. Similar suggestions have been made with grain boundary segregation [25,26]. As the scale grows and thickens, higher stresses are expected. These could change the interface structure, such as destroying its coherency or epitaxy with the underlying alloy [27]. Limited TEM study on γ-Al_2O_3 and α-Al_2O_3 on NiAl [28] has indicated that the interface of the former, the first-formed alumina, was coherent, but incoherent on the latter. It is therefore likely that as the oxide/alloy interface microstructure changed continually with time from coherent to incoherent, it became more accessible to sulfur segregation.

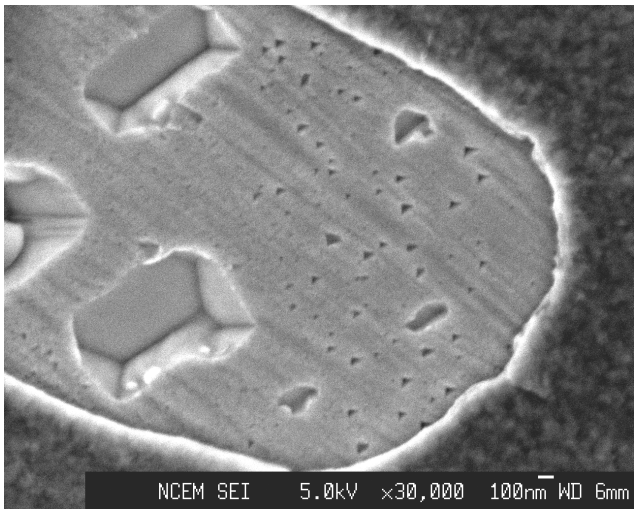

Figure 3: SEM micrograph of a portion of the alloy surface after scale removal, showing different sizes of interfacial pores on an otherwise smooth surface. The oxidation time was 3 minutes.

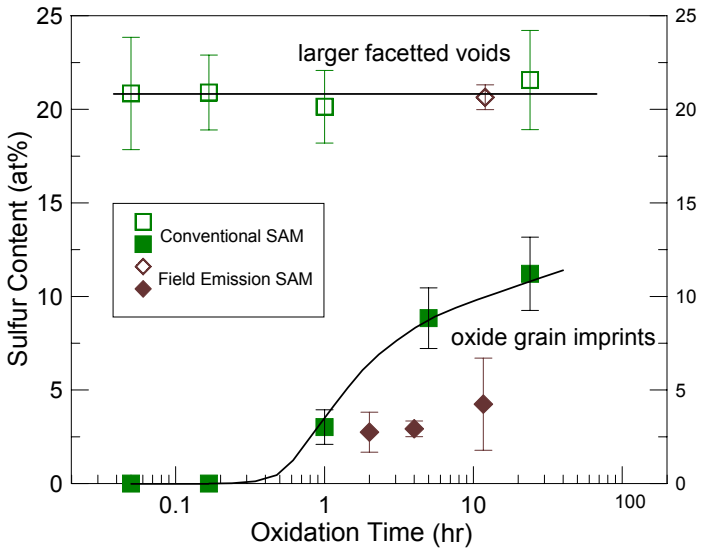

Figure 4: The amount of S on large pore surfaces and on oxide-imprinted areas as a function of oxidation time determined by conventional and FE SAM.

From attenuation of the substrate Fe signal, the amount of S that segregated at the interface was analyzed to be 0.5 monolayer. This level is more than 10 times higher than that calculated from interface sweeping, assuming an entirely inward moving interface [20]. The comparison shows that the detected sulfur was indeed a result of segregation. The amount of sulfur on the large pores was surprisingly high, about 2.5 monolayers. In fact, the larger the pore the higher was the amount of sulfur found on its surface. This relationship is shown in Fig. 5, where S on pore surfaces increased quickly with pore size, then became saturated at 2.5 monolayers on pores larger than about 2 μm. The level of increase is far greater than that expected from gaseous sulfur within the pore that would condense upon cooling. This increase with size is actually a result of S buildup with time, since the average pore size increased with time in relation to the oxide growth rate [23,24]. Concomitant with the increase in S was also an increase in the Al concentration [20], revealing the co-segregation of S and Al to pore surfaces with time.

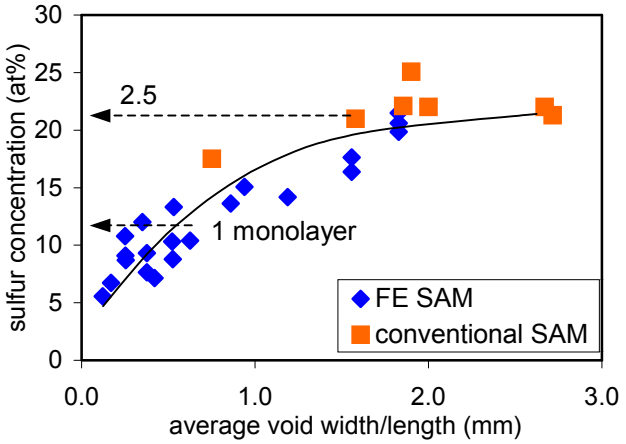

Figure 5: Relationship between interfacial pore size and the amount of sulfur on its surface, as determined from conventional and FE SAM. The high concentration of sulfur resulted from co-segregation with Al.

Impurity Effects on Pore Nucleation and Growth. The coverage of sulfur found on all interfacial pore surfaces seems to support the proposal by Grabke et al [12] that sulfur segregation enhances pore formation. Figure 6 shows a simple schematic of the force balance around the edge of a pore formed at the scale/alloy interface. The energy barrier to nucleate such a pore, ΔG^*, is given by the classical theory of hetero-nucleation [29] as

$$\Delta G^* = \frac{4\pi\gamma_m^3}{3(\Delta G_v^3)}(2+\cos\theta)(1-\cos\theta)^4 \qquad (2)$$

where ΔG_v is the volume free energy change of void nucleation. Since, initially, S only segregated at the pore surface and not at the interface, only γ_m would be affected (S was also never found on the oxide surface). The segregation of S to metal surfaces has been shown to reduce the metal surface energy [30,31]. The degree of reduction depends on the amount of coverage and the S activity. When the coverage is 1 monolayer, γ_m can decrease by 30-50%. This decrease in γ_m will reduce ΔG^* in two ways. The stronger effect is from γ_m^3, and the weaker one from the angle θ dependence, as lower γ_m also decreases θ according to Eqn. 1.

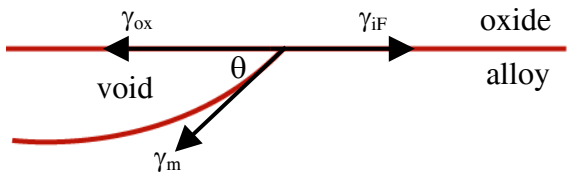

$$\gamma_{iF} = \gamma_{ox} + \gamma_m \cos\theta \qquad (1)$$

Figure 6: Schematic illustration of a pore at the oxide/metal interface and the balance of interfacial and surface energies at the pore edge.

Although the free energy of formation of a pore at the scale/alloy interface can be reduced by the segregation of a surface-energy-lowering impurity such as sulfur, the question to ask is whether sulfur from the alloy can diffuse to the interface fast enough to help nucleate these voids. The reason for such a question is found in Fig. 3, where the oxidation time was as short as 3 minutes and the specimen was still being heated to the desired temperature, but μm-sized pores already existed at the interface. The largest pore on this micrograph measured to be 1.2 μm in length and 0.7 μm in width. AFM results have shown that pore depth was on an average 1/5 of its width and length [23] so this pore should be about 0.14-0.24 μm deep, which is comparable to the scale thickness of ~0.2 μm (Fig. 1). The volume of Al that would be in this void is more than enough to support the sale growth above it. Therefore, these large pores must have nucleated almost as soon as oxidation started while the specimen surface temperature was still quite low. Although S is extremely surface active, its diffusivity is too low below 500°C to allow for noticeable surface coverage [32]. The nucleation of pores during the very initial stage of oxidation must not be affected by sulfur segregation, but may be due to other impurities that were already present at the surface, or perhaps from any carbon impurity in the alloy.

Pores that formed at the scale/alloy interface often appeared in groups; an example is given in Fig. 7(a). It seems that there was some location on the original surface on which pores could form preferentially. These locations were not related to any noticeable surface imperfections, but one possibility could be some kind of surface impurity. To verify this, a dilute $NaNO_3$ solution was placed as droplets onto a polished sample surface prior to oxidation. Areas under the droplets showed much more uniform pore distribution, as seen in Fig. 7(b), and the number density, when evaluated over a

large area, was also higher. This preliminary result shows that Na and/or N impurities on the specimen surface prior to oxidation can enhance interfacial pore nucleation. This can occur with these impurities lowering ΔG^*, in similar ways as S would if segregated at the interface. In this case, segregation from the alloy is no longer required, because the impurity was already present at the metal surface.

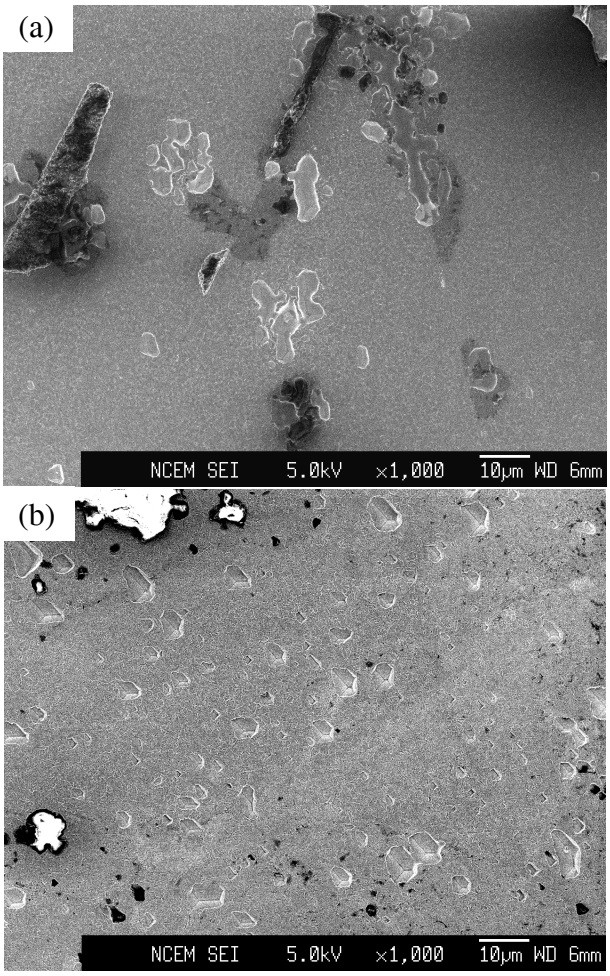

Figure 7: SEM micrograph showing pore formation on the metal surface after oxidation for 1 hr, (a) on untreated alloy surface and (b) on $NaNO_3$ doped surface.

Another possible way the surface impurities can affect pore nucleation may be related to the phenomenon known as impurity induced surface reconstruction [33-36], where a surface impurity can cause significant metal surface faceting or pit formation upon heating to intermediate temperatures, between 70-450°C. The situation is more complicated under oxidizing environments, because a layer of oxide always exists on the metal surface. Initially, it is the native oxide that forms at room temperature. As the metal is heated in oxygen, the oxide quickly thickens and crystallizes. New oxides can also nucleate at the scale/alloy interface. Under these changes, with the details of each process unknown, it is not clear how impurity induced metal surface reconstruction would assist pore formation. Energetically, it would be quite unfavorable for the metal to separate form the oxide to form pits, hence creating new surfaces, unless there is no adhesion between the oxide and the metal. However, on locations where the impurity concentration is high and a strong driving force for pitting or extensive metal surface reconstruction exists, that area may become a preferred site for vacancies to condense out, as a high concentration of them exists at the scale/alloy interface during the growth of the transition alumina. In other words, pore formation during the very initial stage is still considered a result of vacancy condensation. However, instead of a super saturation of vacancies at the interface, which is most likely a good vacancy sink, vacancies are allowed to condense preferentially around surface impurities to help the metal surface establishe its most stable configuration, hence nucleating small voids.

Once pores are nucleated at the interface, they grow in size and depth with continued oxidation. Figure 8 shows a parabolic plot of the average pore size and depth as a function of oxidation time. There are two linear regimes: a faster rate within the first hour and a slower steady state rate afterwards. The transition time corresponds to when a complete layer of α-Al_2O_3 was observed to form at the scale/alloy interface. Using pore volume $=\frac{1}{2}\pi(d/2)^2h$, where d is the pore diameter and h the depth, the initial and steady state pore growth rates are calculated to be 1.8×10^{-6} and 3.0×10^{-7} moles(Al)/cm^{2}h$^{1/2}$ respectively. These values compare well with that calculated from the initial and steady-state oxidation rates, which are 2.5×10^{-6} and 5.2×10^{-7} moles(Al)/cm^{2}h$^{1/2}$ respectively. While smaller pores probably grow by surface diffusion, larger ones are believed to grow by aluminum vapor transport [24].

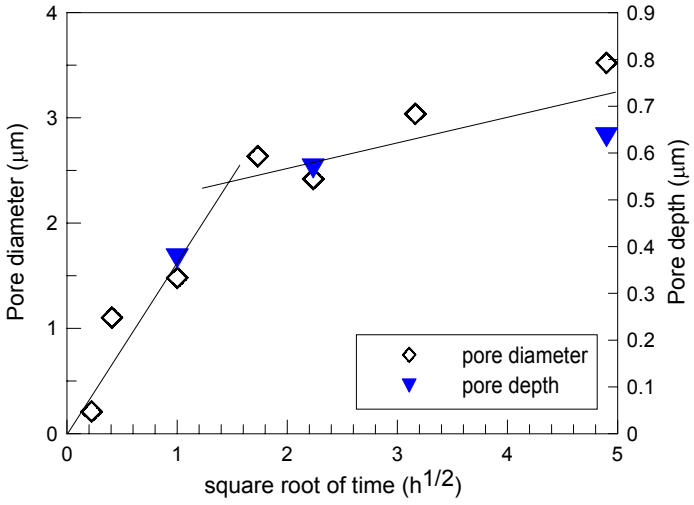

Figure 8: The increase of average pore size and depth with oxidation time.

Pore shape is dominated by the force balance shown in Fig. 6, and by any anisotropy of the surface energies, such that

the simple force balance, equation (1), needs to be modified as [29]

$$\gamma_{iF} + \frac{\delta\gamma_{iF}}{\delta\theta} = \gamma_{ox} + \frac{\delta\gamma_{ox}}{\delta\theta} + \gamma_m \cos\theta + \frac{\delta\gamma_m}{\delta\theta}\sin\theta \qquad (3)$$

where $\delta\gamma/\delta\theta$'s are the changes in surface energy caused by the changes in orientation. Since pores are usually several times larger than the oxide grain size, only the $\delta\gamma_m/\delta\theta$ term in Eqn.3 is important. Alloys whose surface energy is anisotropic should form more facetted voids. As pores grow in size, minimization of its surface area becomes important. This energy requirement causes larger pores to approximate a semi-sphere on the alloy surface; an example is shown in Fig. 9. Although these energy considerations dictate the pore shape, they do not provide any driving force for pore enlargement. The driving force for that must be the oxidation process as Al is constantly transported from the alloy to the scale to maintain scale growth. Since diffusion of Al is faster than Fe in Fe-40Al [37], vacancies from any unequal diffusion will move away from the interface, so pore formation in this case is not expected from the Kirkendall effect.

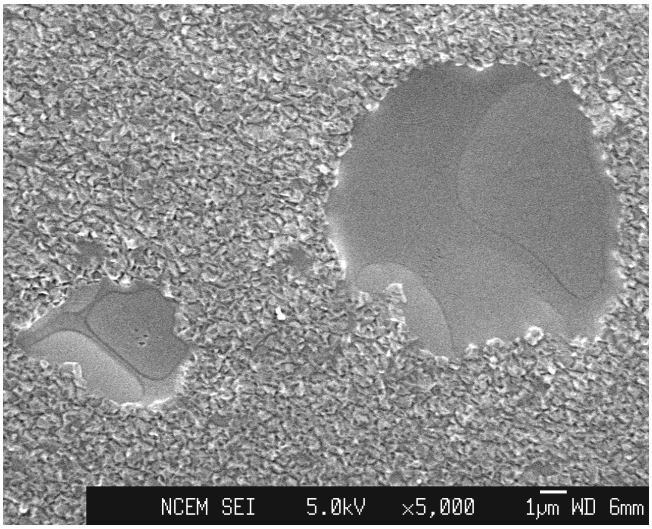

Figure 9: The growth of interfacial pores into a semi-sphere as a way to minimize total surface energy. The scale that formed after 10 hrs spalled during cooling.

The high concentration of sulfur on pore surfaces should have two effects. One is to passivate the surface from being oxidized, hence stabilizing the first formed pores. Sulfur adsorption on metal surfaces is well known to poison the surface from adsorbing other species. This is especially so when the concentration of S is greater than a monolayer [38] as found on the interfacial pores studied here. The second effect is to facilitate pore growth by increasing the metal surface diffusion and enriching the Al content on the pore surface through the co-segregation of S and Al. Grabke et al [30] have reported a 3-fold increase in Fe surface diffusion on S saturated surfaces. The same may be expected with FeAl. This enhanced surface transport rates would be important during the initial stage when the pore size is small [24]. Larger pores grow by Al vapor transport and the higher Al content from co-segregation should enhance this process.

Effect of Reactive Element. There is no extensive void formation when a reactive element (RE), such as Y, Hf or Zr, is present in the alloy [39]. However, voids very similar to that shown in Fig. 3 have been observed by cross-sectional TEM [17] on Y-containing NiAl after 0.1 hrs at 950°C. These voids also showed distinctive facetted sides and bottoms. They were shallow with widths ~ 280 nm and depths ~ 80 nm. The depths were similar to the thickness of the γ-Al_2O_3 scale above them, indicating that they were formed during the very early stage of oxidation, probably influenced by the presence of surface impurities. It is not known whether these voids remained small or continued to grow. The authors [17] suggested that their NiAl alloy did not contain enough Y, and that was why these voids were present. However, the nominal Y content was 0.01wt%, which should be high enough to allow adequate incorporation of Y into the alloy to exert the usual reactive element effect.

Interfacial pores of a different morphology have been reported by Pint on RE containing ODS FeCrAl alloys after longer oxidation times [18,40], i.e., 2 hrs at 1200°C. In these examples, pores a fraction of the size of the oxide grains were present at the scale/alloy interface. Most were located at the junction between two oxide grains and the alloy substrate. The mechanism of pore formation seems different from those initial pores mentioned in the above paragraph. The small pores at grain junctions that remained after a few hours of oxidation most likely appeared during the time α-Al_2O_3 nucleated at the scale/alloy interface. An alloy surface with partially nucleated α-Al_2O_3 grain imprints, after scale removal, is shown in Fig. 10. Many small pores remain between the α-Al_2O_3 grains as they impinge on one another, especially at the junction between 3-4 neighboring grains. These pores may close if there is sufficient lateral growth of the aluminum oxide. Otherwise, they will

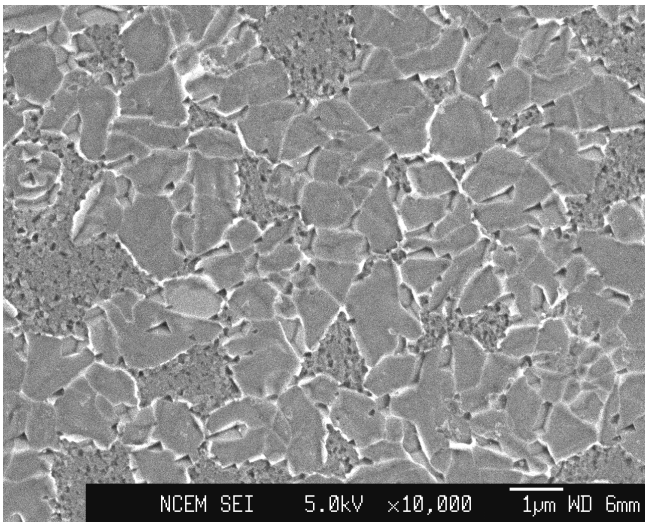

Figure 10: SEM micrograph of the alloy surface after scale removal. The specimen was oxidized for about 1 hr. α-Al_2O_3 grains nucleated at the interface. Small voids are left between the alpha grains as they impinge onto each other.

remain at the interface or become incorporated into the scale as the scale grows inward.

Although for the most part, interfacial pores are not found on reactive element containing alloys, there are examples where pores do exist. The flat, shallow voids reported by Yang et al [17] are particularly interesting. More work should be done to follow the development of these voids with further oxidation, and the experimental uncertainly of how much Y was present in the alloy should be resolved. If surface impurities can indeed enhance pore formation, as suggested by this work, then reactive element containing alloys should be susceptible to that as well unless the presence or RE increases γ_m, thus creating a greater energy barrier for pore nucleation (Eqn. 2). For the small rounded pores observed at the grain junctions, the puzzling question is why they don't grow to larger sizes with continued oxidation. The shape of the voids may be an important factor [40]. A more rounded pore, i.e., larger θ, may be harder to extend along the interface than a flatter, shallower one that is more crack-like. Without the segregated sulfur, surface mobility of Al and Fe on pore surfaces would be slower. This could make the initial pore growth via surface diffusion [24] slower than those that are covered with sulfur on non-RE-containing alloys. One other factor that may be important is that with the presence of a reactive element Al transport through the scale is greatly reduced [41,42]. This means a smaller amount of aluminum vacancies at the scale/alloy interface. The pores that nucleated at the interface are perfect sinks for these vacancies, if they are not already annihilated elsewhere. A decreased vacancy concentration may cause a reduction in the pore growth rate. Furthermore, the inward growth of the Al_2O_3 scale may cause small pores to be incorporated before they can deepen from Al vapor transport, which is expected to take place after the initial oxidation stage as a way of supporting scale growth above the pores [24].

Conclusions

Sulfur from the alloy segregated to Al_2O_3/FeAl interface up to 0.5 monolayer only after a complete layer of α-Al_2O_3 formed at the interface, but the metal side of all interfacial pores was covered with the segregated sulfur at all times. The amount of S on pore surfaces increased with time as pores grew in size to a maximum of ~2.5 monolayers with Al co-segregation. Most pores nucleated at the early stage of oxidation when the scale was mainly the transition phase Al_2O_3. Surface impurities that were present prior to oxidation are believed to contribute to pore formation. Their presence reduces the metal surface energy, hence lowers the free energy of nucleation. The segregated sulfur on pore surfaces facilitate pore growth by enhancing surface diffusion and Al vapor transport. Vacancy condensation at the interface may be the mechanism by which pores are formed, especially at the initial stage when the scale grows mainly by Al outward transport and the scale/alloy interface may be coherent. How reactive elements in the alloy prevent pore formation is still not clear and this is currently being investigated.

Acknowledgment

The author would like to thank Dr. Ian Wright of Oak Ridge National Laboratory for supplying the FeAl alloy. This research was sponsored by the U. S. Department of Energy under contract No. DE-AC03-76SF00098.

References

1. A. Dravnieks and H. J. McDonald, *J. Electrochem. Soc.*, 94, 139-148 (1948).
2. P. S. Dobson and R. E. Smallman, *Proc. R. Soc.,* A293, 423-431 (1966).
3. W. J. Moore, *J. Chem. Phys*., 21, 1117-1123 (1953).
4. R. Hales, R. E. Smallman and P. S. Dobson, *Proc Roy Soc*, A307, 71-81 (1968).
5. D. L. Douglass, *Mat. Sci. Eng*., 3, 255-263 (1969).
6. J. Harris, *Acta Metall*., 26, 1033-1041 (1978).
7. A. Kumar, M. Nasrallah and D. L. Douglass, *Oxid. Met*., 8, 227-263 (1974).
8. D. Caplan, R. J. Hussey, G. I. Sproule, and M. J. Graham, *Oxid. Met*., 14, 279-299 (1980).
9. H. E. Evans, *Mater. Sci. and Tech.*, 4, 1089-1098 (1988).
10. B. Pieraggi, R. A. Rapp, J. P. Hirth, *Oxid. Met*., 44, 63-79 (1995).
11. J. Stringer, *Werk. Korros.*, 23, 747-755 (1972).
12. H. J. Grabke, D. Wiemer and H. Viefhaus, *Appl. Surf. Sci*., 47, 243-250 (1991).
13. M. C. Stasik, F. S. Pettit, G. H. Meier, S. Ashary, and J. L. Smialek, *Scr. Metall. Mater*., 31, 1645-1650 (1994).
14. P. Y. Hou and J. L. Smialek, *Mater. High Temp.***,** 17, 79-85 (2000).
15. A. W. Funkenbusch, J. G. Smeggil, and N. S. Bornstein, *Metall. Trans. A***,** 16A, 1164-1165 (1985).
16. P. Y. Hou, *Oxid. Metals*, 52, 337-351 (1999).
17. J. C. Yang, K. Nadarzinski, E. Schumann and M. Rühle, *Scripta Met*, 33, 1043-48 (1995).
18. B. A. Pint, A. J. Garratt-Reed and L. W. Hobbs, *Mater. High Temp.*, 13, 3-16 (1995).
19. P. Y. Hou, *Mater. Sci. Forum*, 369-372, 23-38 (2001).
20. P. Y. Hou and John Moskito, "FESAM study of sulfur distribution on Al_2O_3/FeAl interfaces", submitted to *Oxid. Met.,* June 2002.
21. E. Shumann, G. Schnotz, K. P. Trumble and M. Ruhle, *Acta metal. mater*., 40, 1311-19 (1992).
22. K. F. McCarty, *Surf. Sci.*, 474, L165-72 (2001).
23. P. Y. Hou, C. Van Leiden, Y. Niu and F. Gesmundo, *High Temperature Corrosion and Materials Chemistry III*, E. J. Opila, M. J. McNallan, D. A. Shores, D. A. Shifler (eds), pp. 15-28, PV 2001-12, the Electrochem Soc. 2001.
24. P. Y. Hou, Y. Niu and C. Van Lienden, *Oxid. Met*., 59, 41-61 (2003).

25. R. W. Balluffi, *Interfacial Segregation*, W. C. Johnson and J. M. Blakely (eds), pp. 193-237, ASM, Metals Park, Ohio, 1997.
26. J. D. Rittner, D. Udler, D. N. Seidman and Y. Oh, *Phys. Rev. Lett*., 74, 1115-1118 (1995).
27. P. Y. Hou, M. J. Bennett and M. Ruhle, *Oxid. Met.* 45, 529-620, (1996).
28. J. C. Yang, E. Schumann, I. Levin and M. Rühle, 46, 2195-2201 (1998).
29. D. P. Woodruff, *The Solid-Liquid Interface*, Cambridge University Press, pp. 15-38, 1973.
30. H. J. Grabke, E. M. Petersen and S. R. Srinivasan, *Surf. Sci*., 67, 501-516 (1977).
31. R. M. Cannon, E. Saiz, A. P. Tomsia and W. C. Carter, "*Structure and Properties of Interfaces in Ceramics*", 279-292, Materials Research Society (USA), 1995.
32. H. J. Grabke, W. Paulitschke, G. Tauber and H. Viefhaus, *Surf. Sci.*, 63, 377-389 (1977).
33. D. P. Woodruff, *J. Phys. Condens. Matter*., 6, 6067-6094 (1994).
34. J. S. Lin, H. Cabibil and J. A. Kelber, *Surf. Sci.*, 395, 30-42 (1998).
35. L. Schwenger and H-J. Ernst, *Surf. Sci.*, 347, 25-32 (1996).
36. J. Guan, R. A. Campbell, T. E. Madey, *Surf. Sci.*, 341, 311-327 (1995).
37. M. Eggermann and H. Meher, *Phil. Mag. A*, 80, 1219-1225 (2000).
38. H. Cabibil, J. S. Lin, and J. A. Kelber, *Surf. Sci.* 382, L645-L651 (1997).
39. D. P. Whiltte and J. Stringer, *Phi. Trans. Roy. Soc. London*, A27, 309-328 (1979).
40. B. Pint, *Oxid. Met.,* 48, 303-328 (1997).
41. W. J. Quadakkers, A. Elschner, W. Speier and H. Nickel, *Appl. Surf. Sci.*, 52, 271-87 (1991).
42. B. A. Pint, J. R. Martin and L. W. Hobbs, *Oxid. Met.*, **39**, 167-95 (1993).